Published in final edited form as:
Exp Neurol. 2007 September ; 207(1): 118–127.

The high affinity peripheral benzodiazepine receptor ligand DAA1106 binds specifically to microglia in a rat model of traumatic brain injury: implications for PET imaging

Sriram Venneti[1], **Amy K. Wagner**[2,3], **Guoji Wang**[1], **Susan L. Slagel**[4], **Xiangbai Chen**[2,3], **Brian J. Lopresti**[4], **Chester A. Mathis**[4], and **Clayton A. Wiley.**[1]

1 *Department of Pathology, University of Pittsburgh School of Medicine, Pittsburgh, Pennsylvania 15213, USA*

2 *Department of Physical Medicine and Rehabilitation, University of Pittsburgh School of Medicine, Pittsburgh, Pennsylvania 15213, USA*

3 *Safar Center for Resuscitation Research, Pittsburgh, Pennsylvania 15213, USA*

4 *Department of Radiology, University of Pittsburgh School of Medicine, Pittsburgh, Pennsylvania 15213, USA*

Abstract

Traumatic brain injury (TBI) is a significant cause of mortality, morbidity, and disability. Microglial activation is commonly observed in response to neuronal injury which, when prolonged, is thought to be detrimental to neuronal survival. Activated microglia can be labeled using PK11195, a ligand that bind the peripheral benzodiazepine receptor (PBR), receptors which are highly expressed in activated microglia and sparse in the resting brain. We compared the binding properties of two PBR ligands PK11195 and DAA1106 in rats using the controlled cortical impact (CCI) model of experimental TBI. While both ligands showed relative increases with specific binding in the cortex ipsilateral to injury compared to the contralateral side, [^{3}H]DAA1106 showed higher binding affinity compared with [^{3}H](R)-PK11195. Combined immunohistochemistry and autoradiography in brain tissues near the injury site showed that [^{3}H]DAA1106 binding co-registered with activated microglia more than astrocytes. Further, increased [^{3}H]DAA1106 specific binding positively correlated with degree of microglial activation, and to a lesser degree with reactive astrocytosis. Finally, *in vivo* administration of each ligand in rats with TBI showed greater retention of [^{11}C]DAA1106 compared to [^{11}C](R)-PK11195 at the site of the contusion as assessed by *ex vivo* autoradiography. These results in a rat model of TBI indicate that [^{11}C]DAA1106 binds with higher affinity to microglia when compared with PK11195, suggesting that [^{11}C]DAA1106 may represent a better ligand than [^{11}C](R)-PK11195 for *in vivo* PET imaging of activated microglia in TBI.

Keywords

Peripheral Benzodiazepine receptor; Microglia; PET imaging; traumatic brain injury; DAA1106; PK11195

Corresponding author: Dr. Clayton A. Wiley, Presbyterian University Hospital, Neuropathology Division, 200 Lothrop Street A515, Pittsburgh, PA, USA 15213. Phone: (412) 647-0765. FAX: (412) 647-5602. Email address: wiley1@pitt.edu

Introduction

With an annual incidence of 200/100,000, traumatic brain injury (TBI) is a major cause of mortality as well as chronic functional impairment and disability in survivors. An estimated two percent of the general population live with cognitive, behavioral, emotional, and physical disabilities (7,57) related to TBI. While several studies have focused on acute neuronal cell death with respect to dissecting mechanisms of injury and designing neuroprotective strategies, glial responses to injury and their influence on neuronal damage and repair are less understood. One of the central glial responses to brain injury is activation of microglia (25,55). However, the role of activated microglia in TBI is largely unknown. Recent evidence using two photon microscopy imaging of fluorescently labeled microglia in transgenic mice following laser-induced injury showed rapid movement of ramified microglial processes to the site of injury. These processes then fused to form an area of containment between healthy and injured tissues within about 30 seconds, suggesting that microglia may represent the first line of defense in CNS injury (15,21,38). Activated microglia also serve phagocytic functions in clearing up debris created by dead cells at the site of brain injury (32). In contrast to these beneficial functions, chronically activated microglia are hypothesized to promote neuronal damage by secreting several neurotoxins, which are thought to trigger various cellular processes including cell death cascades in neurons (54). In humans with TBI, microglial activation has been reported as early as 72 hours after injury (20), and can remain activated for up to several weeks after injury (5). In a rodent model of TBI chronic microglial activation is noted up to two weeks after CCI (48). However, it is not known if this prolonged activation of microglia in TBI can be harmful and detrimental to the reparative process. If microglial activation could be effectively evaluated *in vivo*, it would be possible to identify dynamic neuroinflammatory changes as well as monitor efficacy of therapies targeted at modulating neuroinflammation in TBI.

Activated microglia show increased expression of the peripheral benzodiazepine receptor PBR), which unlike the central benzodiazepine receptor, is expressed at relatively low levels in the normal brain on resting microglia and astrocytes (9,10). PK11195 a pharmacological ligand that binds to PBR has been used to label activated microglia in brain tissues in a number of neurologic diseases (1) including a rat model of TBI (48). Carbon-11 labeled PK11195 has been used as a PET imaging agent and shows increased uptake to varying degrees (compared to control subjects) in human patients with several neurological disorders such as stroke (22, 24,47,49), multiple sclerosis (3,16,60), Alzheimer's disease (8), amyotrophic lateral sclerosis (58), Parkinson's disease (23,40) and Huntington's disease (43).

DAA1106 ([N-(2,5-dimethoxybenzyl)-N-(4-uoro-2-phenoxyphenyl) acetamide]), is a more recently discovered PBR ligand that binds with higher affinity compared to PK11195 as demonstrated by a significantly lower dissociation constant (K_D) (11,34,64). Due to its high affinity binding properties, it has been suggested that DAA1106 may provide greater sensitivity than PK11195 as a PET imaging agent for PBR. The higher affinity of DAA1106 may also overcome the low specific *in vivo* binding signal with PK11195, which is challenging to quantify with typical PET image noise levels (3,26,41,45). Carbon-11 labeled DAA1106 has been shown to cross the blood brain barrier and bind to constitutive PBR in normal human subjects (29). However, the binding characteristics of DAA1106 in conditions of CNS pathology are not known. Further, it is not known if DAA1106 preferentially labels activated microglia in conditions of CNS injury such as TBI. To address these questions we a used controlled cortical impact injury (CCI) model of TBI in rats. We report that [^{3}H]DAA1106 displays higher binding affinity compared to [^{3}H](R)-PK11195 in injured brain tissue obtained from rats seven days after CCI. Increases in [^{3}H]DAA1106 binding correlated mainly to activated microglia. While [^{3}H](R)-PK11195 has been shown to bind to activated microglia in brain tissues in a rat model of TBI (48), we now show that both [^{11}C](R)-PK11195 and

[^{11}C]DAA1106 can bind *in vivo* to activated microglia using *ex vivo* autoradiography. Further our data suggest that microglia in rats with TBI bind and retain more DAA1106 compared to PK11195 in rats with TBI and may serve as a better ligand to image brain microglia *in vivo* using PET in brain injury.

Methods

Animal model of TBI using controlled cortical impact injury (CCI)

Animals were housed and maintained according to standards of the Association for Assessment and Accreditation of Laboratory Animal Care, and all experiments were approved by the University of Pittsburgh Institutional Animal Care and Use Committee. Ten male adult male rats (Hilltop laboratories, Scottdale PA), with body weight 280–320g were initially anesthetized with 4% isoflurane and a 2:1 N_2O/O_2 mixture in a vented anesthesia chamber. Following endotracheal intubation, rats were mechanically ventilated with a 2% isoflurane mixture. The rats were then mounted in a stereotaxic frame (David Kopf instruments, Tujunga, CA). Following a craniotomy, the CCI was delivered at 2.9mm; 4m/s over the right parietal cortex similar to that previously described (30,31,62). Following CCI, animals were allowed to recover and were housed for 7 days. Four animals were imaged with *ex vivo* autoradiography and six animals were used for filtration binding analyses and immunohistochemistry. Following deep anesthesia with isoflurane, animals were sacrificed, and brain tissues from all animals were collected and processed to 1) obtain frozen sections for immunohistochemistry/ autoradiography, 2) obtain homogenates for filtration binding assays and 3) obtain sections for *ex vivo* autoradiography.

The CCI device used in this study has been described in detail by Dixon (18). In brief, the CCI injury device consists of a small (1.975 cm) bore, double-acting stroke-constrained pneumatic cylinder with a 5.0 cm stroke. The cylinder is rigidly mounted on a crossbar at an 18-degree angle and has an impact tip of 6mm mounted on the lower rod. The upper rod end is attached to the transducer core of a linear velocity displacement transducer (LVDT). The impactor tip is pneumatically driven at a predetermined velocity, depth, and duration of tissue deformation. The velocity of the cylinder is controlled by gas pressure and measured directly by the LVDT. A penetration depth of 2.9 mm with a velocity of 4.0 m/sec consistently produces a severe injury.

Filtration radioligand binding assays

Cortical brain tissue from the right parietal cortex containing the core of the contusion and 5 mm around the core along with brain tissue from left parietal cortex corresponding to the region of contusion on the contralateral side were rapidly dissected out and homogenized in 50 mM HEPES (4°C, pH 7.4). Homogenates (total protein concentration ranging from 150 to 200 μg) were incubated with either 0.5–64 nM [^{3}H](R)-PK11195 (n=3) (sp. act., 89.9 Ci/mmol; NEN Life Sciences Products, Boston, MA) or 0.2 to 20 nM [^{3}H]-DAA1106 (n=3) (sp. act., 80 Ci/mmol; American Radiolabeled Chemical, St Louis, MO) at 4°C for 2 hr in a final volume of 250 μl of HEPES. This was defined as total binding. Nonspecific binding was determined by the inclusion of 10 μM PK11195 or 10 μM DAA11106 respectively in parallel samples. The reaction was terminated in a vacuum cell harvester (Brandel, Gaithersburg, MD) by filtration through glass fiber filters (Whatman- GF/B glass fiber filter paper) presoaked in 0.3% polyethyleneimine (Sigma, St. Louis, MO) by the addition of ice-cold HEPES. Filter bound radioactivity was counted in a liquid scintillation spectrometer (Tricarb liquid scintillation counter, Perkin Elmer Life Sciences, Wellesley, MA) after the addition of 6 mls of liquid scintillation fluid (Perkin Elmer Life Sciences). Specific binding at each concentration of ^{3}H-ligand was defined as the difference between total binding and nonspecific binding and ranged from 80–90% of total binding. All samples were run in duplicate. Bmax in fmoles per mg

protein measuring the maximal number of binding sites for each ligand was taken to reflect the total number of receptors and K_D, the dissociation constant reported in nM and inversely proportional to the binding affinity of the ligand were determined for each ligand using PRISM software (Graphpad, San Diego, CA). The $Bmax/K_D$ indicative of the binding potential for PET radiotracers (36)was calculated for each ligand.

Immunohistochemistry

Immunostaining and laser confocal microscopic imaging was performed on frozen sections of obtained from the same animals used for filtration binding analyses in a manner similar to that described previously (59). Frozen sections obtained from rats with CCI were stained with antibodies to GFAP (mouse monoclonal, DAKO, Carpinteria, CA), or anti-rat CD68 (mouse monoclonal, Serotec, Raleigh, NC), or NeuN (mouse monoclonal, Zymed/Invitrogen, Carlsbad, CA) used at concentrations 1:1000, 1:100 and 1:50 respectively. Sections were then incubated with Cy5- or Cy3-conjugated anti-mouse IgG at a concentration of 1:200 (Jackson Immunoresearch Laboratories Inc., West Grove, PA). Immunostained sections were then scanned and quantified on a laser confocal microscope equipped with an argon laser with 458 nm, 477 nm, 488 nm and 514 nm primary emission lines. (LSM 510, Zeiss, Heidelberg, Germany) as described in detail elsewhere (59). Briefly, each section was scanned along the *z*-axis to define the middle optical plane used in quantification (262,144 pixels/plane; 1 pixel= 0.25 μm^2). Image analysis was performed on a Silicon Graphics computer (Windows NT 4.0 operating system, Microsoft, Redmond, Washington) using the LSM software (version 3.0, Zeiss). Scanning parameters such as laser power aperture, gain, and photomultiplier tube settings were kept constant for each wavelength. An individual blinded to the experimental design imaged three areas in the core of the lesion and three areas in the corresponding contralateral region (40X) encompassing 106,100 μm^2. For each cell phenotype scanned, contribution to signal intensity from autofluorescence was minimized using a threshold that was kept constant. In each area the average pixel fluorescence, along with the pixel counts for a given cell phenotype marker that exceeded the threshold, were enumerated. The average pixel fluorescence was multiplied by the total number of pixels to represent the total florescence for that cell phenotype marker in that area. The total fluorescence values determined from the three scanned areas in one brain region were averaged to represent a measure of the cell phenotype in that brain region.

In vitro Autoradiography

Autoradiography was performed as described earlier (59). Briefly, 15 μm thick frozen brain sections placed on Superfrost™ glass slides (Sigma) were incubated in ice-cold 50 mM TRIS-HEPES (pH 7.4) containing (1 nM [^{3}H](R)-PK11195) or 1 nM [^{3}H]DAA1106 for 30 min. Specificity of binding was ensured by the inclusion of 1 μM PK11195 or 1 μM DAA1106 in parallel sections. The sections were mounted with a layer of autoradiographic LM-1 emulsion (Amersham, UK), were developed after 4 weeks and were then imaged on the confocal microscope. Cellular localization of [^{3}H]DAA1106 in brain sections from CCI rats was evaluated by combining immunostaining and autoradiography. Sections were first immunostained with both GFAP and CD68 or NeuN as above and then processed for autoradiography with [^{3}H]DAA1106, following which they were imaged on the confocal microscope.

Ex-vivo autoradiography

High specific activity [^{11}C](R)-PK11195 and [^{11}C]DAA1106 was synthesized at the University of Pittsburgh PET Facility using methods similar to those previously described (59,64). In brief, [^{11}C](R)-PK11195 was labeled with carbon-11 with methylation performed at room temperature to minimize the dechlorination side reaction (13,52). [^{11}C]DAA1106 was

labeled with carbon-11 by O-[^{11}C] methylation of a desmethyl precursor (DAA1123) (64). Chemical and radiochemical purities were ≥95% with specific activities ≥2.0 Ci/μmol at the end of a 40 min synthesis. Typical end-of-synthesis yields were approximately 30% for both [^{11}C]DAA1106 and [^{11}C](R)-PK11195

Anesthetized rats with CCI were injected intravenously through the tail vein with either [^{11}C] DAA1106 (n=2) or [^{11}C](R)-PK11195 (n=2) (750 -1500 μCi). After a 30 min uptake period, animals were perfused with normal saline, sacrificed, and the brain was rapidly removed and placed on a chilled sectioning block (Harvard Apparatus, Natick, MA). The brain was sectioned coronally into 2mm sections and sections taken through the core of the contusion were mounted on a plastic film and opposed to a phosphor screen (Fuji BAS-SR2025, Fuji Photo Film Co., Kanagawa, Japan) for 1 h, after which the exposed plated was imaged on a high-resolution phosphorimager (Fuji BAS-5000, Fuji Medical Systems, Stamford, CT). Images were pseudo colored and scaled to a rainbow scale using the Multi Gauge software (Fuji Medical Systems, Stamford, CT).

Statistical analysis

Data were analyzed using PRISM software (Graphpad, San Diego, CA). Data are represented as mean ± SEM. Student's *t* tests with 95% confidence intervals were used to analyze data from filtration binding experiments and immunohistochemical quantifications. Nonparametric correlational analyses using 95% confidence intervals were performed to quantify the relationship between [^{3}H]DAA1106 binding and microglia (CD68 staining) or astrocytes (GFAP staining). Results from correlational analyses are represented by *r*, the Spearman's coefficient.

Results

[^{3}H]DAA1106 shows increased binding at the site of the contusion in a rat model of TBI

We examined the binding characteristics of DAA1106 and PK11195 in a rat model of TBI using CCI. Saturation filtration binding experiments were performed in rats with CCI using cortical tissues taken from the contusion core and from the corresponding region contralateral to the injury site using [^{3}H]DAA1106 (n=3) and [^{3}H](R)-PK11195 (n=3), (Figure 1). The Bmax (fmols/mg), reflective of the total number of binding sites, was significantly higher with [^{3}H](R)-PK11195 in the contusion compared with cortical tissue contralateral to the contusion (Figure 1B and C, $p = 0.0488$). These results are in agreement with a previous study evaluating [^{3}H](R)-PK11195 binding in rats with CCI after seven days (48). [^{3}H]DAA1106 similarly showed a significant increase in Bmax in the area ipsilateral to the contusion compared the contralateral area (Figure 1A and C, $p = 0.0109$). Within the same region, [^{3}H](R)-PK11195 binding was higher than [^{3}H]DAA1106 binding, approaching significance in the ipsilateral area (Figure 1C, $p = 0.0742$), but not the contralateral area ($p = 0.1331$).

[^{3}H]DAA1106 shows lower K_D values and higher Bmax/K_D ratios compared to [^{3}H](R)-PK11195 in brain tissue obtained from rats with TBI

The K_D (nM), reflective of the ligand binding affinity was measured with both ligands in the ipsilateral and contralateral regions. Comparing ipsilateral and the contralateral regions, the K_D did not different with either [^{3}H]DAA1106 ($p = 0.1835$) or [^{3}H]-(R)PK11195 ($p = 0.6664$) (Figure 1D). However, the K_D of [^{3}H]DAA1106 was significantly lower (~ 4 fold) than with that of [^{3}H]-(R)PK11195 in both ipsillateral ($p = 0.0400$) and contralateral ($p = 0.0125$) regions.

The ratio of Bmax/K_D, employed as an index of binding potential of PET radiotracers, was calculated with each ligand in the ipsilateral and contralateral regions. Bmax/K_D ratio was significantly higher with [^{3}H]DAA1106 on the ipsilateral compared to the contralateral side

($p = 0.0395$). Further, Bmax/K_D ratio was significantly higher (~5 fold higher) for [^{3}H] DAA1106 compared to [^{3}H]-(R)PK11195 on the ipsilateral side ($p = 0.0094$), suggesting that the binding potential of [^{3}H]DAA1106 was higher than [^{3}H]-(R)PK11195 at the site of the lesion.

[^{3}H]DAA1106 binding corresponds to activated microglia in rats with TBI

We determined the relative contributions of astrocytes and microglia to [^{3}H]DAA1106 bindings as PBR is expressed mainly on these cells in the CNS (3,10). We combined immunostaining for astrocytes (GFAP) and activated microglia (CD68) with [^{3}H]DAA1106 autoradiography on frozen brain sections obtained from rats with TBI. [^{3}H]DAA1106 binding co-registered with activated microglia more than GFAP labeled astrocytes in the region of the contusion (Figure 2 A). Minimal [^{3}H]DAA1106 binding as well as CD68 staining was observed in cortical regions in the contralateral hemisphere (Figure 2B). [^{3}H]DAA1106 binding was confirmed to be specific as it was displaced by unlabeled DAA1106 (1 μM) in the region of the contusion in adjacent sections (Figure 2C).

We next quantified the degree of microglial activation using CD68 and the degree of reactive astrocytosis using GFAP in frozen sections obtained from the same rat brain tissue used for filtration binding analyses and correlated these values with [^{3}H]DAA1106 Bmax values. CD68 and GFAP immunohistochemistry were both significantly higher in the contusion compared to contralateral tissue (Figure 3 A–C) [^{3}H]DAA1106 binding correlated with the abundance of microglia (Figure 3D, r=0.8989, p=0.0148), but not with the abundance of astrocytes (Figure 3E, r=0.5385, p=0.2703). These results suggest that the predominant cellular component of DAA1106 binding in the injured CNS relates to activated microglia.

[^{3}H]DAA1106 binding is higher in regions with neuronal loss

To assess the relationship between [^{3}H]DAA1106 binding and neuronal loss we combined [^{3}H]DAA1106 autoradiography with immunostaining for neurons (NeuN) on frozen brain sections obtained from rats with CCI. Increased [^{3}H]DAA1106 binding was observed in association with decreased NeuN staining in areas of the contusion (Figure 4 A). [^{3}H]DAA1106 binding was confirmed to be specific as it was displaced by unlabeled DAA1106 (1 μM) in the ipsilateral (Figure 4B) and contralateral regions in adjacent sections (Figure 4C).

Ex-vivo binding analysis shows increased brain retention of [^{11}C]DAA1106 compared to [^{11}C](R)-PK11195 in rats with TBI

[^{11}C]DAA1106 or [^{11}C](R)-PK11195 was injected intravenously into rats with CCI (n=4, 2 per ligand). While both ligands showed increased ipsilateral retention in the area of the contusion, [^{11}C]DAA1106 retention was qualitatively higher compared to [^{11}C](R)-PK11195 at the site of the contusion (Figure 5 A and B). These results are consistent with the filtration binding studies, suggesting that DAA1106 has higher binding affinity, reflected by the lower K_D and higher Bmax/K_D ratio (a measure of the binding potential) compared to PK11195 in rats with CCI *in vivo.*

Discussion

TBI is a significant cause of disability resulting in a variety of deficits due to neuronal damage (7,57). In response to neuronal injury, microglia undergo a transformation from a resting state to an activated state that is reflected by both morphologic and phenotypic changes (46). While it has been suggested that activated microglia represent a marker for neuronal damage, the role of activated microglia in TBI is not well defined (55). We sought to label activated microglia in the CCI model of TBI in rats. Activated microglia have been imaged *in vivo* using PET by taking advantage of increased expression of PBR, which is normally expressed at low levels

in astrocytes and resting microglia (8,10). PK11195, a ligand that specifically binds to PBR, has been used extensively to image activated microglia using PET in a number of neurologic disorders (reviewed in (9). Further, [^{3}H](R)-PK11195 has been used to label microglia in a rat model of TBI in brain tissues (48), but it not known if ligands that bind PBR can label microglia in TBI *in vivo*. DAA1106 is a new ligand that binds to PBR with higher affinity than PK11195 in brain mitochondrial preparations (11). We now show that the higher affinity of DAA1106 compared to PK11195 translates to superior *in vivo* labeling of microglia using *ex vivo* autoradiography.

In this study, we compared the binding characteristics of DAA1106 with PK11195 and elucidated the cell type contributing to DAA1106 binding in rats with CCI. Filtration binding analyses showed that the dissociation constant (K_D) of [3H]DAA1106 was 5–10 fold lower than [^{3}H](R)-PK11195 in rats with TBI, reflecting a significantly higher binding affinity to PBR (Figures 1). The Bmax, which reflects the number of binding sites, was lower with [^{3}H] DAA1106 than [^{3}H](R)-PK11195 in the area of the contusion and approached statistical significance (Figure 1, p=0.0742). This approximate two-fold difference may be due to a difference in binding sites of either ligand to the peripheral benzodiazepine receptor as detailed in previous reports suggesting that the binding domains of PK11195 and DAA1106 do not completely overlap (14,39). However, despite this two-fold difference in Bmax, the ratio of Bmax to K_D, a measure of specific binding of PET radiotracers (36), was substantially (approximately five fold) higher with [^{3}H]DAA1106 than [^{3}H](R)-PK11195 (Figure 1), suggesting that DAA1106 possesses advantageous features as a PET ligand compared to (R)-PK11195. [^{3}H]DAA1106 bound better to activated microglia and to a lesser degree to astrocytes as determined by combined autoradiography and immunohistochemistry (Figure 2) and correlational analyses (Figure 3). Immunostaining for neurons combined with autoradiography showed that neurons did not colocalize with [^{3}H]DAA1106 binding, but regions within the contusion and with neuronal loss showed greater [^{3}H]DAA1106 labeling (Figure 4). *In vivo* administration of each of the ligands in rats with TBI showed increased brain retention of [^{11}C]DAA1106 compared to [^{11}C](R)-PK11195 at the site of the lesion as assessed by *ex-vivo* autoradiography (Figure 5). Taken together, these data suggest that DAA1106 is a specific marker for activated microglia, which may better delineate activated microglia due to its higher binding affinity when compared to PK11195, in TBI.

Microglia represent a major cellular component of the brain that modulate inflammatory processes (32). However, microglia are sensitive to a variety of neuronal stressors including injury and degenerative processes. Inflammation of the CNS is a ubiquitous component to brain injury, which can be mediated by intrinsic microglia. The role of activated microglia in influencing neuronal injury and repair in TBI is poorly understood. Activated microglia migrate to the area where damage to neural tissue has occurred, where they proliferate and mediate the inflammatory response. Indeed, recent studies suggest that glial activation occurs in both excitotoxic (17,19) and TBI models (28), and reactive microglia play a role in complement activation following TBI (4). Chronically activated microglia as sources of neurotoxins have been hypothesized to exacerbate neuronal injury (6). However, recent investigations suggest that activated microglial cell function may paradoxically support both a neurotoxic and neuroprotective role in the injured brain (56). Polazzi's review suggests that neurons and microglia dynamically interact and communicate through cytokines and chemotactant factors to activate microglia, to attract them to areas of neuronal dysfunction and damage, to minimize the local neurotoxic effects of apoptotic neurons through phagocytosis, and to provide anti-inflammatory and neurotrophic support to sublethally injured and surrounding uninjured neurons (46). Some literature suggests that microglia derived neurotrophic factors can protect metabolically impaired neurons in culture (42) and that microglia facilitate axonal regrowth and sprouting after CNS injury (46). *In vivo* evaluation of microglial activation using PET may help better understand the role played by these cells in TBI.

The specific cell contributions to PBR binding in neuroinflammation are subject to debate. A strong correlation with [^{3}H](R)-PK11195 binding and activated microglia detected by immunohistochemical staining with ED1 has been reported in a rat model of CCI (48). This study also reports a lesser correlation with [^{3}H](R)-PK11195 binding and GFAP labeled astrocytes (48). Our results suggesting that [^{3}H]DAA1106 binds mainly to activated microglia and to a lesser degree with astrocytes in a rat model of TBI are similar to these results obtained with [^{3}H](R)-PK11195 (48). The neurotoxins trimethyltin (33) and cuprizone (12) when administered to rats show increased astrocyte binding of [^{3}H](R)-PK11195 following an initial increase in microglia. However, other studies report good correspondence between [^{3}H](R)-PK11195 binding and activated microglia in rat models of stroke (37), ischemia (53) and facial nerve axotomy (2), experimental autoimmune encephalitis (61), multiple sclerosis (3,61), macaques models of HIV encephalitis (35,59), and hippocampal lesions in mice (44) similar to the data reported in this study.

Microglial activation has been imaged using PET in human subjects with [^{11}C](R)-PK11195 in a variety of neurologic disorders (9). [^{11}C](R)-PK11195 retention in these studies is generally observed in regions of the brain associated with the presence of neuroinflammation. However, [^{11}C](R)-PK11195 retention is also observed in regions not associated with disease specific pathology and neuroinflammtion such as the thalamus in Alzheimer's disease (8) and Parkinson's disease (40), and the occipital cortex in amyotrophic lateral sclerosis (58). Since it is not possible to confirm presence of activated microglia by histological in these regions in human studies, it is possible that these findings reflect regional variations in the constitutive PBR population that are independent of the disease pathology or a non-uniform element of non-specific [^{11}C](R)-PK11195 binding. Further, the extent of activation of microglia to be present in the CNS before a signal can be detected may be low using [^{11}C](R)-PK11195 suggestive of low sensitivity. For example, no significant differences are noted in [^{11}C](R)-PK11195 PET imaging in HIV infected patients with or without dementia (27,63) and between controls and patients diagnosed with mild cognitive impairment (50,51), a condition that may progress to Alzheimer's disease. Therefore, it is possible that the high affinity of DAA1106 to PBR present in activated microglia may represent a significant improvement in specificity and sensitivity over PK11195. We are currently examining DAA1106 imaging in macaques infected with lentiviruses, rats injected with 6-OHDA to model Parkinson's disease and rats injected with lipopolysaccaride to model neuroinflammation. These studies will address the utility of DAA1106 to localize microglial activation in other models CNS injury that have modest to severe levels of microglial activation.

Our *in vivo* studies comparing both ligands were restricted to *ex vivo* autoradiographic analyses due to constraints of the relatively small size of the rodent brain and limited resolution of the PET systems. Further, in rats with CCI [^{3}H](R)-PK11195 binding is observed in areas that project to the area of contusion such as the hippocampus and the thalamus (48). While retention of [^{11}C]DAA1106 was higher on the ipsilateral side compared with [^{11}C](R)-PK11195, we were unable to draw any conclusions regarding DAA1106 binding in areas that project to the site of lesion due to the limited resolution of *ex vivo* autoradiography. Despite these limitations, rodent systems provide us the flexibility and ease to assess pharmacological properties of potential PET ligands as well as provide immunohistochemical analyses which suggest that [^{3}H]DAA1106 has a significantly higher binding potential than [^{3}H](R)-PK11195 and corresponds mainly to activated microglia. We are currently examining the binding properties of [^{11}C]DAA1106 *in vivo* using PET in macaque models where these limitations are more easily circumvented. However, our data suggesting that DAA1106 exhibits many favorable properties including high binding affinity and cellular localization to activated microglia in brain tissues, could potentially represent improvements over PK11195 in the delineation of activated microglia *in vivo* using PET in TBI. It is not known if ligands that bind PBR can label activated microglia *in vivo* in TBI. Our data in a rats with CCI suggest that while both [^{11}C]

(R)-PK11195 and [^{11}C]DAA1106 label activated microglia *in vivo*, the higher binding affinity of characteristics of [^{11}C]DAA1106 make it a potentially viable ligand for clinical studies in TBI. Further longitudinal studies in human subjects with and without TBI are needed to fully characterize the potential enhancements of [^{11}C]DAA1106 and to determine if this ligand is sensitive to measure changes in neuroinflammation over time. These studies may also help illuminate the role of activated microglia in TBI and their responses to anti-inflammatory therapies.

Acknowledgements

We thank James Kasenchak and Jason Nugyen for technical help and James Ruskiewicz for help with the PET scans. This work was supported by the National Institutes of Health RO1 MH64921 (CAW), K24 MH01717 (CAW) and K08HD40833 (AKW).

References

1. Banati RB. Visualising microglial activation in vivo. Glia 2002;40:206–217. [PubMed: 12379908]
2. Banati RB, Myers R, Kreutzberg GW. PK ('peripheral benzodiazepine')--binding sites in the CNS indicate early and discrete brain lesions: microautoradiographic detection of [3H]PK11195 binding to activated microglia. J Neurocytol 1997;26:77–82. [PubMed: 9181482]
3. Banati RB, Newcombe J, Gunn RN, Cagnin A, Turkheimer F, Heppner F, Price G, Wegner F, Giovannoni G, Miller DH, Perkin GD, Smith T, Hewson AK, Bydder G, Kreutzberg GW, Jones T, Cuzner ML, Myers R. The peripheral benzodiazepine binding site in the brain in multiple sclerosis: quantitative in vivo imaging of microglia as a measure of disease activity. Brain 2000;123 (Pt 1):2321–2337. [PubMed: 11050032]
4. Bellander BM, Bendel O, Von Euler G, Ohlsson M, Svensson M. Activation of microglial cells and complement following traumatic injury in rat entorhinal-hippocampal slice cultures. J Neurotrauma 2004;21:605–615. [PubMed: 15165368]
5. Beschorner R, Nguyen TD, Gozalan F, Pedal I, Mattern R, Schluesener HJ, Meyermann R, Schwab JM. CD14 expression by activated parenchymal microglia/macrophages and infiltrating monocytes following human traumatic brain injury. Acta Neuropathol (Berl) 2002;103:541–549. [PubMed: 12012085]
6. Block ML, Zecca L, Hong JS. Microglia-mediated neurotoxicity: uncovering the molecular mechanisms. Nat Rev Neurosci 2007;8:57–69. [PubMed: 17180163]
7. Bontke, CFBC. Principles of Brain Injury Rehabilitation. In: RL, B., editor. Physical Medicine and Rehabilitation. W.B. Saunders Company; Philadelphia, PA: 1996. p. 1027-1051.
8. Cagnin A, Brooks DJ, Kennedy AM, Gunn RN, Myers R, Turkheimer FE, Jones T, Banati RB. In-vivo measurement of activated microglia in dementia. Lancet 2001;358:461–467. [PubMed: 11513911]
9. Cagnin A, Gerhard A, Banati RB. In vivo imaging of neuroinflammation. Eur Neuropsychopharmacol 2002;12:581–586. [PubMed: 12468021]
10. Casellas P, Galiegue S, Basile AS. Peripheral benzodiazepine receptors and mitochondrial function. Neurochem Int 2002;40:475–486. [PubMed: 11850104]
11. Chaki S, Funakoshi T, Yoshikawa R, Okuyama S, Okubo T, Nakazato A, Nagamine M, Tomisawa K. Binding characteristics of [3H]DAA1106, a novel and selective ligand for peripheral benzodiazepine receptors. Eur J Pharmacol 1999;371:197–204. [PubMed: 10357257]
12. Chen MK, Baidoo K, Verina T, Guilarte TR. Peripheral benzodiazepine receptor imaging in CNS demyelination: functional implications of anatomical and cellular localization. Brain 2004;127:1379–1392. [PubMed: 15069023]
13. Cleij, MCAF.; Baron, JC.; Clark, JC. Base-promoted dechlorination of (R)-[C-11]PK-11195. 15th International Symposium on Radiopharmaceutical Chemistry; 2003. p. 588
14. Culty M, Silver P, Nakazato A, Gazouli M, Li H, Muramatsu M, Okuyama S, Papadopoulos V. Peripheral benzodiazepine receptor binding properties and effects on steroid synthesis of two new phenoxyphenyl-acetamide derivatives, DAA1097 and DAA1106. Drug Development Research 2001;52:475–484.

15. Davalos D, Grutzendler J, Yang G, Kim JV, Zuo Y, Jung S, Littman DR, Dustin ML, Gan WB. ATP mediates rapid microglial response to local brain injury in vivo. Nat Neurosci 2005;8:752–758. [PubMed: 15895084]

16. Debruyne JC, Versijpt J, Van Laere KJ, De Vos F, Keppens J, Strijckmans K, Achten E, Slegers G, Dierckx RA, Korf J, De Reuck JL. PET visualization of microglia in multiple sclerosis patients using [11C]PK11195. Eur J Neurol 2003;10:257–264. [PubMed: 12752399]

17. Dihne M, Block F, Korr H, Topper R. Time course of glial proliferation and glial apoptosis following excitotoxic CNS injury. Brain Res 2001;902:178–189. [PubMed: 11384611]

18. Dixon CE, Clifton GL, Lighthall JW, Yaghmai AA, Hayes RL. A controlled cortical impact model of traumatic brain injury in the rat. J Neurosci Methods 1991;39:253–262. [PubMed: 1787745]

19. Dommergues MA, Plaisant F, Verney C, Gressens P. Early microglial activation following neonatal excitotoxic brain damage in mice: a potential target for neuroprotection. Neuroscience 2003;121:619–628. [PubMed: 14568022]

20. Engel S, Schluesener H, Mittelbronn M, Seid K, Adjodah D, Wehner HD, Meyermann R. Dynamics of microglial activation after human traumatic brain injury are revealed by delayed expression of macrophage-related proteins MRP8 and MRP14. Acta Neuropathol (Berl) 2000;100:313–322. [PubMed: 10965802]

21. Fetler L, Amigorena S. Neuroscience. Brain under surveillance: the microglia patrol. Science 2005;309:392–393. [PubMed: 16020721]

22. Gerhard A, Neumaier B, Elitok E, Glatting G, Ries V, Tomczak R, Ludolph AC, Reske SN. In vivo imaging of activated microglia using [11C]PK11195 and positron emission tomography in patients after ischemic stroke. Neuroreport 2000;11:2957–2960. [PubMed: 11006973]

23. Gerhard A, Pavese N, Hotton G, Turkheimer F, Es M, Hammers A, Eggert K, Oertel W, Banati RB, Brooks DJ. In vivo imaging of microglial activation with [11C](R)-PK11195 PET in idiopathic Parkinson's disease. Neurobiol Dis 2006;21:404–412. [PubMed: 16182554]

24. Gerhard A, Schwarz J, Myers R, Wise R, Banati RB. Evolution of microglial activation in patients after ischemic stroke: a [11C](R)-PK11195 PET study. Neuroimage 2005;24:591–595. [PubMed: 15627603]

25. Giordana MT, Attanasio A, Cavalla P, Migheli A, Vigliani MC, Schiffer D. Reactive cell proliferation and microglia following injury to the rat brain. Neuropathol Appl Neurobiol 1994;20:163–174. [PubMed: 8072646]

26. Groom GN, Junck L, Foster NL, Frey KA, Kuhl DE. PET of peripheral benzodiazepine binding sites in the microgliosis of Alzheimer's disease. J Nucl Med 1995;36:2207–2210. [PubMed: 8523106]

27. Hammoud DA, Endres CJ, Chander AR, Guilarte TR, Wong DF, Sacktor NC, McArthur JC, Pomper MG. Imaging glial cell activation with [11C]-R-PK11195 in patients with AIDS. J Neurovirol 2005;11:346–355. [PubMed: 16162478]

28. Igarashi T, Huang TT, Noble LJ. Regional vulnerability after traumatic brain injury: gender differences in mice that overexpress human copper, zinc superoxide dismutase. Exp Neurol 2001;172:332–341. [PubMed: 11716557]

29. Ikoma Y, Yasuno F, Ito H, Suhara T, Ota M, Toyama H, Fujimura Y, Takano A, Maeda J, Zhang MR, Nakao R, Suzuki K. Quantitative analysis for estimating binding potential of the peripheral benzodiazepine receptor with [(11)C]DAA1106. J Cereb Blood Flow Metab 2007;27:173–184. [PubMed: 16685259]

30. Kline AE, Massucci JL, Marion DW, Dixon CE. Attenuation of working memory and spatial acquisition deficits after a delayed and chronic bromocriptine treatment regimen in rats subjected to traumatic brain injury by controlled cortical impact. J Neurotrauma 2002;19:415–425. [PubMed: 11990348]

31. Kline AE, Yan HQ, Bao J, Marion DW, Dixon CE. Chronic methylphenidate treatment enhances water maze performance following traumatic brain injury in rats. Neurosci Lett 2000;280:163–166. [PubMed: 10675786]

32. Kreutzberg GW. Microglia: a sensor for pathological events in the CNS. Trends Neurosci 1996;19:312–318. [PubMed: 8843599]

33. Kuhlmann AC, Guilarte TR. Cellular and subcellular localization of peripheral benzodiazepine receptors after trimethyltin neurotoxicity. J Neurochem 2000;74:1694–1704. [PubMed: 10737628]

34. Maeda J, Suhara T, Zhang MR, Okauchi T, Yasuno F, Ikoma Y, Inaji M, Nagai Y, Takano A, Obayashi S, Suzuki K. Novel peripheral benzodiazepine receptor ligand [11C]DAA1106 for PET: An imaging tool for glial cells in the brain. Synapse 2004;52:283–291. [PubMed: 15103694]
35. Mankowski JL, Queen SE, Tarwater PJ, Adams RJ, Guilarte TR. Elevated peripheral benzodiazepine receptor expression in simian immunodeficiency virus encephalitis. J Neurovirol 2003;9:94–100. [PubMed: 12587072]
36. Mintun MA, Raichle ME, Kilbourn MR, Wooten GF, Welch MJ. A quantitative model for the in vivo assessment of drug binding sites with positron emission tomography. Ann Neurol 1984;15:217–227. [PubMed: 6609679]
37. Myers R, Manjil LG, Cullen BM, Price GW, Frackowiak RS, Cremer JE. Macrophage and astrocyte populations in relation to [3H]PK 11195 binding in rat cerebral cortex following a local ischaemic lesion. J Cereb Blood Flow Metab 1991;11:314–322. [PubMed: 1997503]
38. Nimmerjahn A, Kirchhoff F, Helmchen F. Resting microglial cells are highly dynamic surveillants of brain parenchyma in vivo. Science 2005;308:1314–1318. [PubMed: 15831717]
39. Okuyama S, Chaki S, Yoshikawa R, Ogawa S, Suzuki Y, Okubo T, Nakazato A, Nagamine M, Tomisawa K. Neuropharmacological profile of peripheral benzodiazepine receptor agonists, DAA1097 and DAA1106. Life Sci 1999;64:1455–1464. [PubMed: 10321725]
40. Ouchi Y, Yoshikawa E, Sekine Y, Futatsubashi M, Kanno T, Ogusu T, Torizuka T. Microglial activation and dopamine terminal loss in early Parkinson's disease. Ann Neurol 2005;57:168–175. [PubMed: 15668962]
41. Pappata S, Levasseur M, Gunn RN, Myers R, Crouzel C, Syrota A, Jones T, Kreutzberg GW, Banati RB. Thalamic microglial activation in ischemic stroke detected in vivo by PET and [11C]PK1195. Neurology 2000;55:1052–1054. [PubMed: 11061271]
42. Park LC, Zhang H, Gibson GE. Co-culture with astrocytes or microglia protects metabolically impaired neurons. Mech Ageing Dev 2001;123:21–27. [PubMed: 11640948]
43. Pavese N, Gerhard A, Tai YF, Ho AK, Turkheimer F, Barker RA, Brooks DJ, Piccini P. Microglial activation correlates with severity in Huntington disease: a clinical and PET study. Neurology 2006;66:1638–1643. [PubMed: 16769933]
44. Pedersen MD, Minuzzi L, Wirenfeldt M, Meldgaard M, Slidsborg C, Cumming P, Finsen B. Up-regulation of PK11195 binding in areas of axonal degeneration coincides with early microglial activation in mouse brain. Eur J Neurosci 2006;24:991–1000. [PubMed: 16930426]
45. Petit-Taboue MC, Baron JC, Barre L, Travere JM, Speckel D, Camsonne R, MacKenzie ET. Brain kinetics and specific binding of [11C]PK 11195 to omega 3 sites in baboons: positron emission tomography study. Eur J Pharmacol 1991;200:347–351. [PubMed: 1782994]
46. Polazzi E, Contestabile A. Reciprocal interactions between microglia and neurons: from survival to neuropathology. Rev Neurosci 2002;13:221–242. [PubMed: 12405226]
47. Price CJ, Wang D, Menon DK, Guadagno JV, Cleij M, Fryer T, Aigbirhio F, Baron JC, Warburton EA. Intrinsic activated microglia map to the peri-infarct zone in the subacute phase of ischemic stroke. Stroke 2006;37:1749–1753. [PubMed: 16763188]
48. Raghavendra Rao VL, Dogan A, Bowen KK, Dempsey RJ. Traumatic brain injury leads to increased expression of peripheral-type benzodiazepine receptors, neuronal death, and activation of astrocytes and microglia in rat thalamus. Exp Neurol 2000;161:102–114. [PubMed: 10683277]
49. Ramsay SC, Weiller C, Myers R, Cremer JE, Luthra SK, Lammertsma AA, Frackowiak RS. Monitoring by PET of macrophage accumulation in brain after ischaemic stroke. Lancet 1992;339:1054–1055. [PubMed: 1349076]
50. Schuitemaker A, Van Berckel BN, Boellaard R, Kropholler M, Boellaard R, Jonker C, Lubberlink M, Scheltens P, Lammertsma AA. Assessment of microglial activation in mild cognitive impairment using [11C](R)-PK11195 and PET. Neuroimage 2006;31:T159.
51. Schuitemaker A, Van Berckel BN, Kropholler M, Boellaard R, Jonker C, Scheltens P, Lammertsma AA. Microglia activation in mild cognitive impairment. Neurobiol of Aging 2004;25(Suppl 2):S286.
52. Shah F, Hume SP, Pike VW, Ashworth S, McDermott J. Synthesis of the enantiomers of [N-methyl-11C]PK 11195 and comparison of their behaviours as radioligands for PK binding sites in rats. Nucl Med Biol 1994;21:573–581. [PubMed: 9234314]

53. Stephenson DT, Schober DA, Smalstig EB, Mincy RE, Gehlert DR, Clemens JA. Peripheral benzodiazepine receptors are colocalized with activated microglia following transient global forebrain ischemia in the rat. J Neurosci 1995;15:5263–5274. [PubMed: 7623150]

54. Stoll G, Jander S. The role of microglia and macrophages in the pathophysiology of the CNS. Prog Neurobiol 1999;58:233–247. [PubMed: 10341362]

55. Streit WJ. The role of microglia in brain injury. Neurotoxicology 1996;17:671–678. [PubMed: 9086488]

56. Streit WJ. Microglial response to brain injury: a brief synopsis. Toxicol Pathol 2000;28:28–30. [PubMed: 10668987]

57. Thurman DJ, Alverson C, Dunn KA, Guerrero J, Sniezek JE. Traumatic brain injury in the United States: A public health perspective. J Head Trauma Rehabil 1999;14:602–615. [PubMed: 10671706]

58. Turner MR, Cagnin A, Turkheimer FE, Miller CC, Shaw CE, Brooks DJ, Leigh PN, Banati RB. Evidence of widespread cerebral microglial activation in amyotrophic lateral sclerosis: an [11C](R)-PK11195 positron emission tomography study. Neurobiol Dis 2004;15:601–609. [PubMed: 15056468]

59. Venneti S, Lopresti BJ, Wang G, Bissel SJ, Mathis CA, Meltzer CC, Boada F, Capuano S 3rd, Kress GJ, Davis DK, Ruszkiewicz J, Reynolds IJ, Murphey-Corb M, Trichel AM, Wisniewski SR, Wiley CA. PET imaging of brain macrophages using the peripheral benzodiazepine receptor in a macaque model of neuroAIDS. J Clin Invest 2004;113:981–989. [PubMed: 15057304]

60. Versijpt J, Debruyne JC, Van Laere KJ, De Vos F, Keppens J, Strijckmans K, Achten E, Slegers G, Dierckx RA, Korf J, De Reuck JL. Microglial imaging with positron emission tomography and atrophy measurements with magnetic resonance imaging in multiple sclerosis: a correlative study. Mult Scler 2005;11:127–134. [PubMed: 15794383]

61. Vowinckel E, Reutens D, Becher B, Verge G, Evans A, Owens T, Antel JP. PK11195 binding to the peripheral benzodiazepine receptor as a marker of microglia activation in multiple sclerosis and experimental autoimmune encephalomyelitis. J Neurosci Res 1997;50:345–353. [PubMed: 9373043]

62. Wagner AK, Kline AE, Sokoloski J, Zafonte RD, Capulong E, Dixon CE. Intervention with environmental enrichment after experimental brain trauma enhances cognitive recovery in male but not female rats. Neurosci Lett 2002;334:165–168. [PubMed: 12453621]

63. Wiley CA, Lopresti BJ, Becker JT, Boada F, Lopez OL, Mellors J, Meltzer CC, Wisniewski SR, Mathis CA. Positron emission tomography imaging of peripheral benzodiazepine receptor binding in human immunodeficiency virus-infected subjects with and without cognitive impairment. J Neurovirol 2006;12:262–271. [PubMed: 16966217]

64. Zhang MR, Kida T, Noguchi J, Furutsuka K, Maeda J, Suhara T, Suzuki K. [(11)C]DAA1106: radiosynthesis and in vivo binding to peripheral benzodiazepine receptors in mouse brain. Nucl Med Biol 2003;30:513–519. [PubMed: 12831989]

Abbreviations

^{11}C
: Crabon-11 isotope

^{3}H
: Tritium isotope

Bmax
: Maximal bound Receptors

BP
: Binding Potential

CCI
: Controlled Cortical Impact injury

CD68
: Rat lysosomal marker for activated microglia

CNS
Central Nervous System

DAA1106
(N-(2,5-Dimethoxybenzyl)-N-(5-fluoro-2-phenoxyphenyl) acetamide)

GFAP
Glial Fibrillary Acidic Protein (marker for astrocytes)

HIV
Human Immunodeficiency Virus

K_D
Dissociation Constant

Min
Minute

NeuN
Neuron specific Nuclear protein (marker for neurons)

PBR
Peripheral Benzodiazepine Receptor

PET
Positron Emission Tomography

(R)-PK11195
(R)enantiomer of [1-(2-chlorophenyl)-N-methyl-N-(1methylpropyl)-3-isoquinolinecarboxamide]

TBI
Traumatic Brain Injury

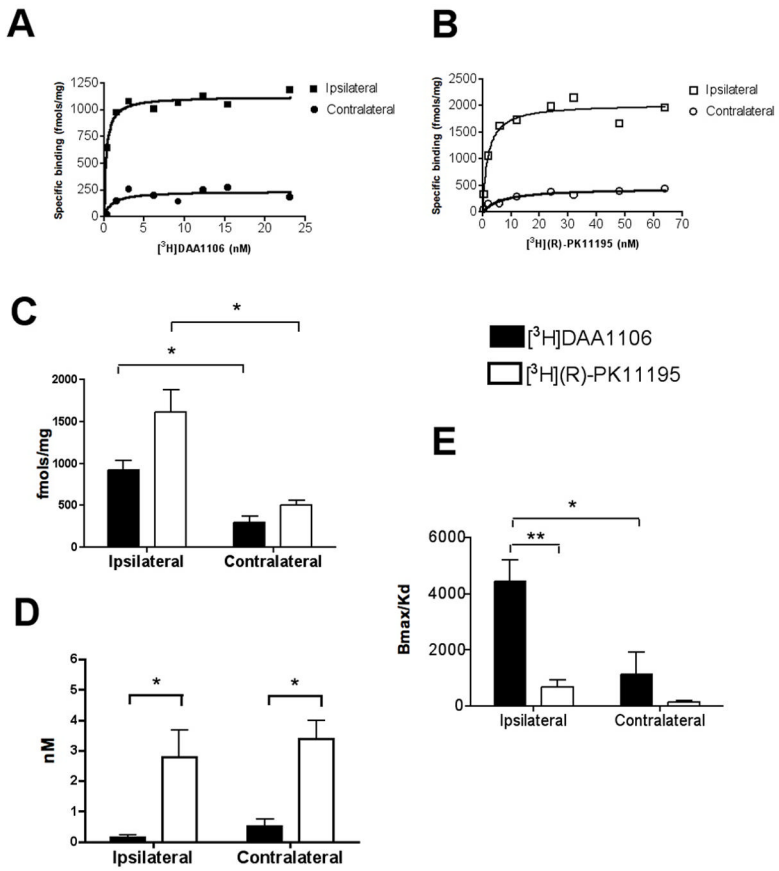

Figure 1. [^{3}H]DAA1106 shows lower K_D values in rats with TBI when compared with [^{3}H](R)-PK11195

Saturation filtration binding experiments were performed in the cortex of rats with CCI on the side ipsilateral and the side contralateral to injury using [^{3}H]DAA1106 (n=3) (black symbols) and [^{3}H](R)-PK11195 (n=3) (open symbols). The Bmax (fmols/mg), reflective of the total number of binding sites and the K_D (nM) reflective of the binding affinity of the ligands to PBR was calculated using PRISM software.

A and B, Representative saturation binding curves with [^{3}H]DAA1106 (**A**) and [^{3}H]-(R) PK11195 (**B**) from rats with CCI in the cortex ipsilateral to (squares) and contralateral (circles) to the contusion.

C, The Bmax (fmols/mg), reflective of the total number of binding sites was significantly higher in the area ipsilateral to the contusion compared with the area contralateral to the contusion with both [^{3}H]DAA1106 (black bars, $p = 0.0109$) and [^{3}H](R)-PK11195 (clear bars, $p = 0.0488$). Bmax with [^{3}H]DAA1106 and [^{3}H](R)-PK11195 did not differ significantly in either the ipsilateral ($p = 0.0742$) or the contralateral ($p = 0.1331$) side to the injury.

D, The K_D (nM), reflective of the ligand binding affinity was not different between the ipsilateral and the contralateral regions with either [^{3}H]DAA1106 ($p = 0.1835$) or [^{3}H]-(R) PK11195 ($p = 0.6664$). However, the K_D with [^{3}H]DAA1106 was significantly lower than with [^{3}H]-(R)PK11195 in both ipsillateral ($p = 0.0400$) and contralateral ($p = 0.0125$) regions.

E, The ratio of Bmax/K_D, representative of the binding potential of each ligand was calculated with each ligand in the ipsilateral and contralateral regions. Bmax/K_D ratio was significantly higher with [^{3}H]DAA1106 on the ipsilateral compared to the contralateral side ($p = 0.0395$). Bmax/K_D ratio was significantly higher with [^{3}H]DAA1106 compared to [^{3}H]-(R)PK11195 on the ipsilateral side ($p = 0.0094$). Data was analyzed using student's *t* test, **p<0.01, *p<0.05.

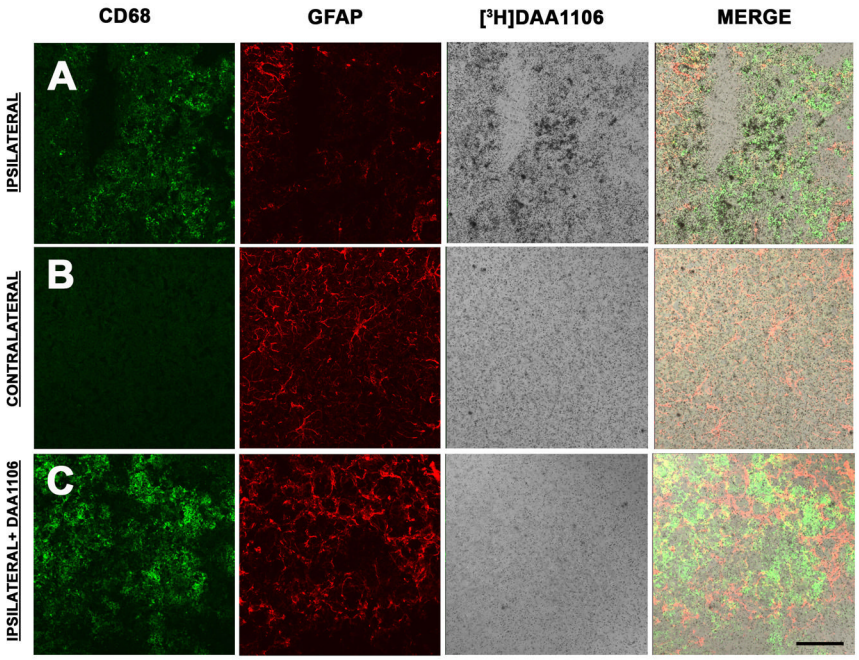

Figure 2. [^{3}H]DAA1106 binding corresponds to microglia in rats with TBI

A–B, Combined [^{3}H]DAA1106 autoradiography (black grains) and immunostaining for activated microglia (CD68, green) and astrocytes (GFAP, red) was performed in cortical brain tissue in rats with CCI on the ipsilateral side at the site of contusion (**A**) and on the contralateral side (**B**). On the ipsilateral side (**A**), [^{3}H]DAA1106 Specific binding overlapped with CD68 labeled microglia but not with GFAP immunostained astrocytes (vertical panel - Merge). On the contralateral side (**B**), minimal CD68 and [^{3}H]DAA1106 binding was seen.

C, [^{3}H]DAA1106 autoradiographic binding was confirmed to be specific as it was displaced by unlabeled DAA1106 in adjacent sections on the ipsilateral side. Scale bar indicates 50 μm.

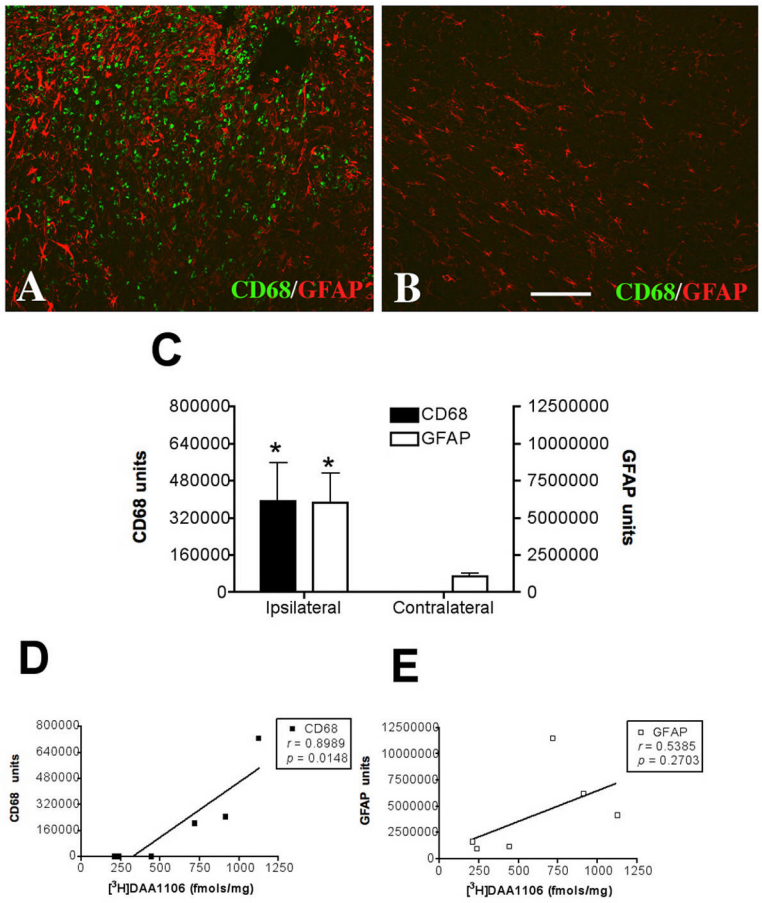

Figure 3. [^{3}H]DAA1106 specific binding correlates with the abundance of activated microglia but not astrocytes

A–B, Combined immunostaining for activated microglia (CD68, green) and astrocytes (GFAP, red) was performed in cortical brain tissue in rats with CCI at the side ipsilateral to the contusion (**A**) and the contralateral side (**B**). The ipsilateral side showed prominent activation of microglia and astrocytosis (**A**) compared to the contralateral side (**B**). Scale bar indicates 50 μm.

C, Activated microglia (CD68, black bars, left Y-axis, p=0.0491) and astrogliosis (GFAP, clear bars, right Y-axis, p=0.04615) were significantly higher on the side ipsilateral to the lesion compared to the contralateral side. Data was analyzed using student's t test, *p<0.05.

D–E, [^{3}H]DAA1106 Specific binding (Bmax, X-axis) correlated with the abundance of microglia (**D**, CD68, black squares, r=0.8989, p=0.0148), but not with the abundance of astrocytes (**E**, GFAP, clear squares, r=0.5385, p=0.2703).

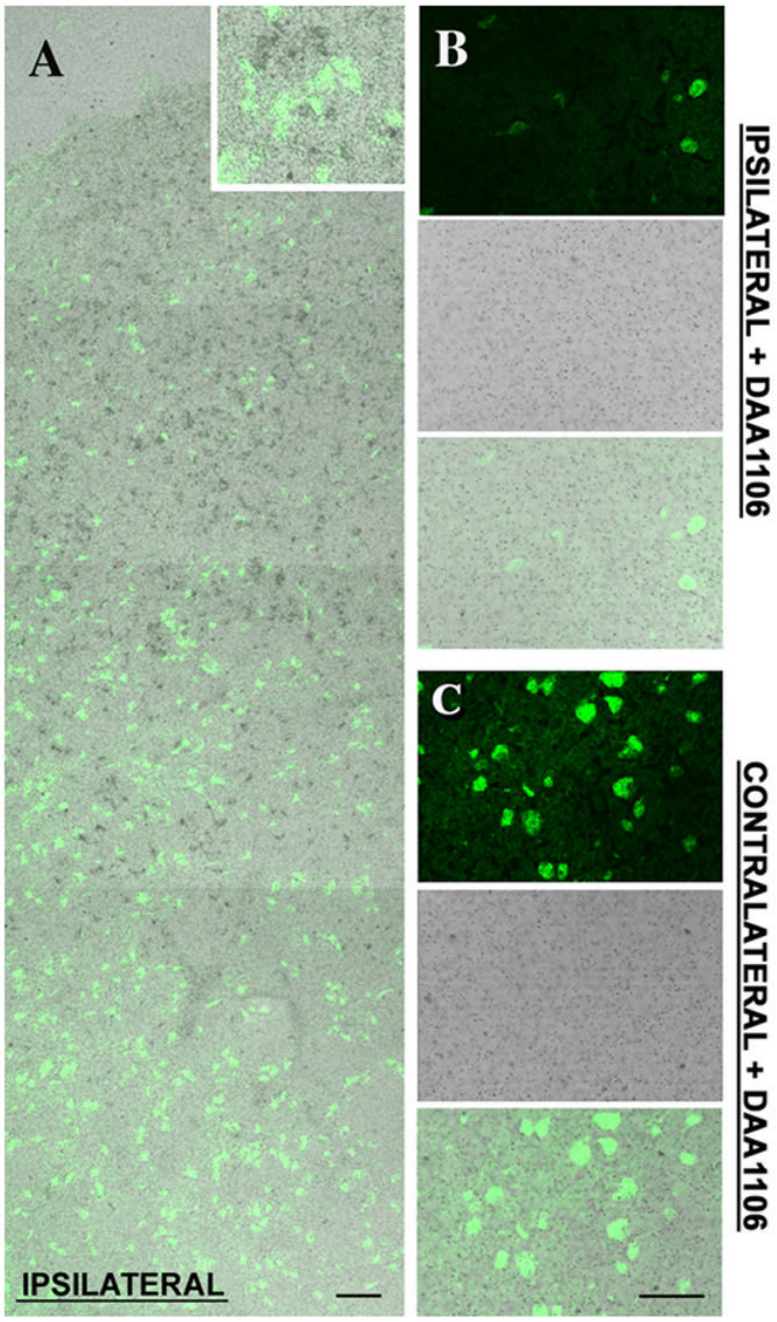

Figure 4. [^{3}H]DAA1106 binding is higher in regions with neuronal loss

A, Montage image of combined NeuN staining (green) and [^{3}H]DAA1106 autoradiography (Black grains) in cortical brain section obtained from rats with CCI. NeuN staining did not overlap with [^{3}H]DAA1106 binding (inset). NeuN staining progressively decreases as the site of the lesion is approached indicating neuronal loss. Scale bar indicates 50 μm.

B & C, [^{3}H]DAA1106 autoradiographic binding was confirmed to be specific on the ipsilateral side (**B**) and on the contralateral side (**C**) as it was displaced by unlabeled DAA1106. Scale bar indicates 50 μm.

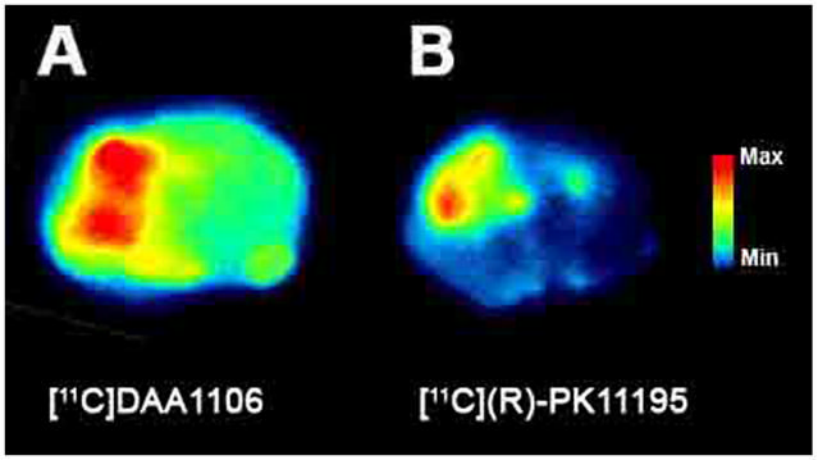

Figure 5. [^{11}C]DAA1106 is retained at greater levels at the site of the lesion compared to [^{11}C](R)-PK11195 in rats with TBI

Rats with CCI were injected with either [^{11}C]DAA1106 or [^{11}C](R)-PK11195 (1–2mCi) intravenously. A 30-minute uptake period was allowed after radiotracer injection, following which animals were sacrificed and brain tissue was processed for *ex-vivo* autoradiography. Uptake of [^{11}C]DAA1106 at the site of lesion (**A**) is greater than [^{11}C](R)-PK11195 uptake (**B**).